

Supplementary Materials to

# Automated seafloor massive sulfide detection through integrated image segmentation and geophysical data analysis: Revisiting the TAG hydrothermal field

Amir Haroon<sup>1,2</sup>, Hendrik Paasche<sup>3</sup>, Sebastian Graber<sup>1,4</sup>, Sven Petersen<sup>1</sup>, Eric Attias<sup>5,6</sup>, Marion Jegen<sup>1</sup>, Romina Gehrman<sup>7</sup>, Sebastian Hölz<sup>1</sup>, Meike Klischies<sup>1,8</sup>

<sup>1</sup> Helmholtz Centre for Ocean Research, GEOMAR Kiel, Wischhofstr. 1-3, 24148, Kiel Germany

<sup>2</sup> Hawaii Institute of Geophysics and Planetology, School of Ocean and Earth Science and Technology, University of Hawai'i at Manoa, Honolulu, HI, USA

<sup>3</sup> UFZ Helmholtz Centre for Environmental Research, Leipzig, Germany

<sup>4</sup> Helmut-Schmidt Uni Hamburg

<sup>5</sup> Institute for Geophysics, Jackson School of Geosciences, The University of Texas at Austin, Austin, TX, USA

<sup>6</sup> Department of Geology and Geophysics, Woods Hole Oceanographic Institution, Woods Hole, Massachusetts, USA

<sup>7</sup> Defence Research and Development Canada, Dartmouth, NS, Canada

<sup>8</sup> North.io GmbH, Einsteinstraße 1, 24118 Kiel, Germany

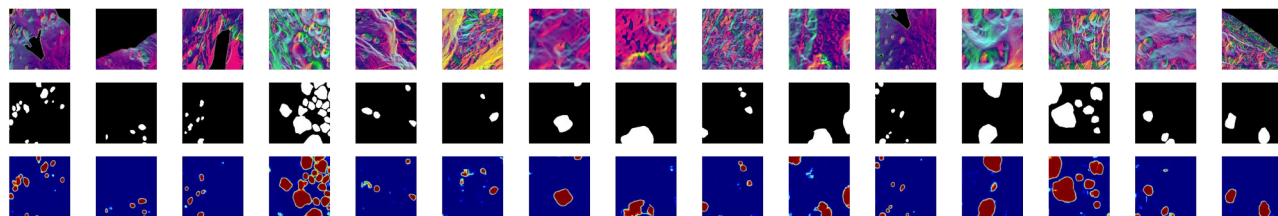
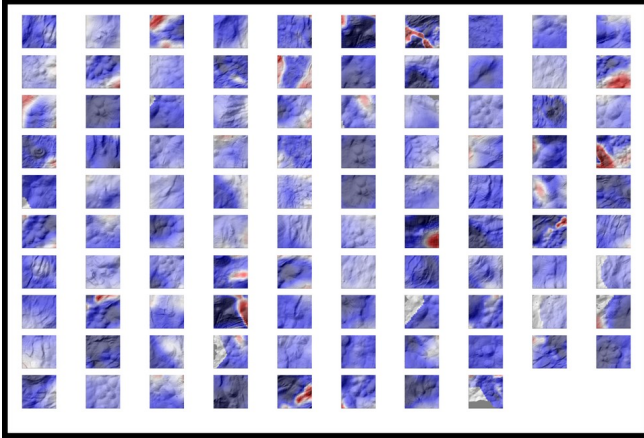
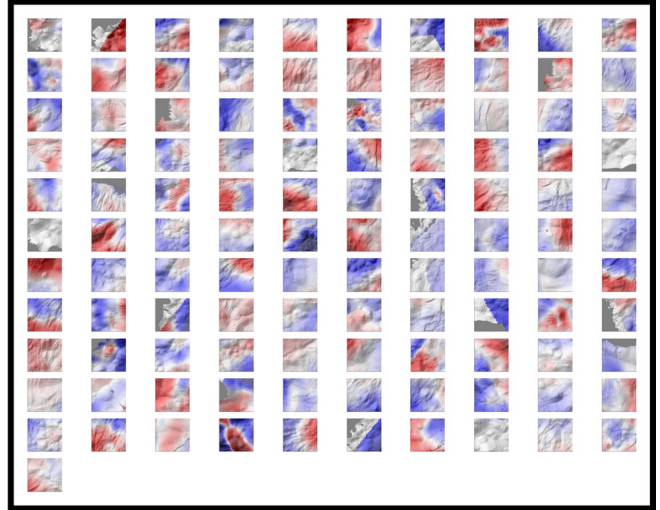


*Figure S1: Suite of 15 randomly chosen test images (top row), corresponding manual annotations (middle row) and U-Net predictions (bottom row). The upper row represents the pre-processed image, the middle row the manually labeled masks illustrated as a binary image (either 0 or 1) where regions associated to mounds are white and background regions are black. The bottom row displays the pixel affiliations as probabilities. Blue regions are low and red regions denote high probability of the corresponding pixel belonging to a mound structure. The prediction images use cold coloring to depict zero or low probabilities, whereas hot coloring corresponds to an increased or high probability of each pixel's mound affiliation. Overall, the trained network detects and outlines the majority of the annotated mounds efficiently and in certain instances, may detect mounds that were manually annotated incorrectly. Other instances show that the network may incorrectly segment mounds located at the image edges or, in very few cases, miss manually labeled mounds located in the image center.*

Cluster 1



Cluster 2



Cluster 3

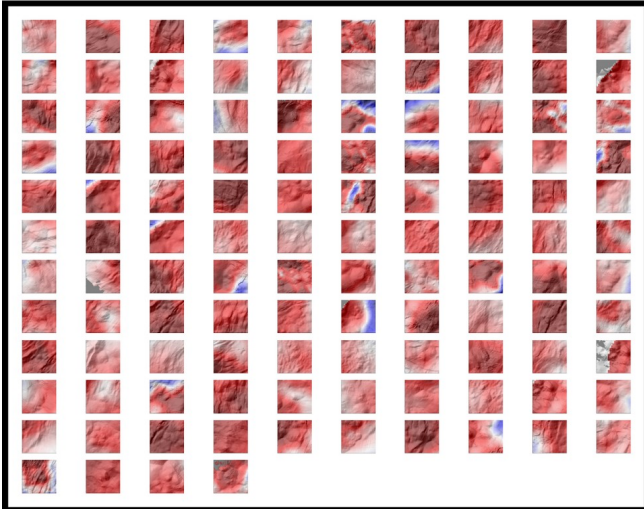


Figure S2: Images of the individual mounds clustered into each group as overlays of magnetic anomaly and hillshade bathymetry

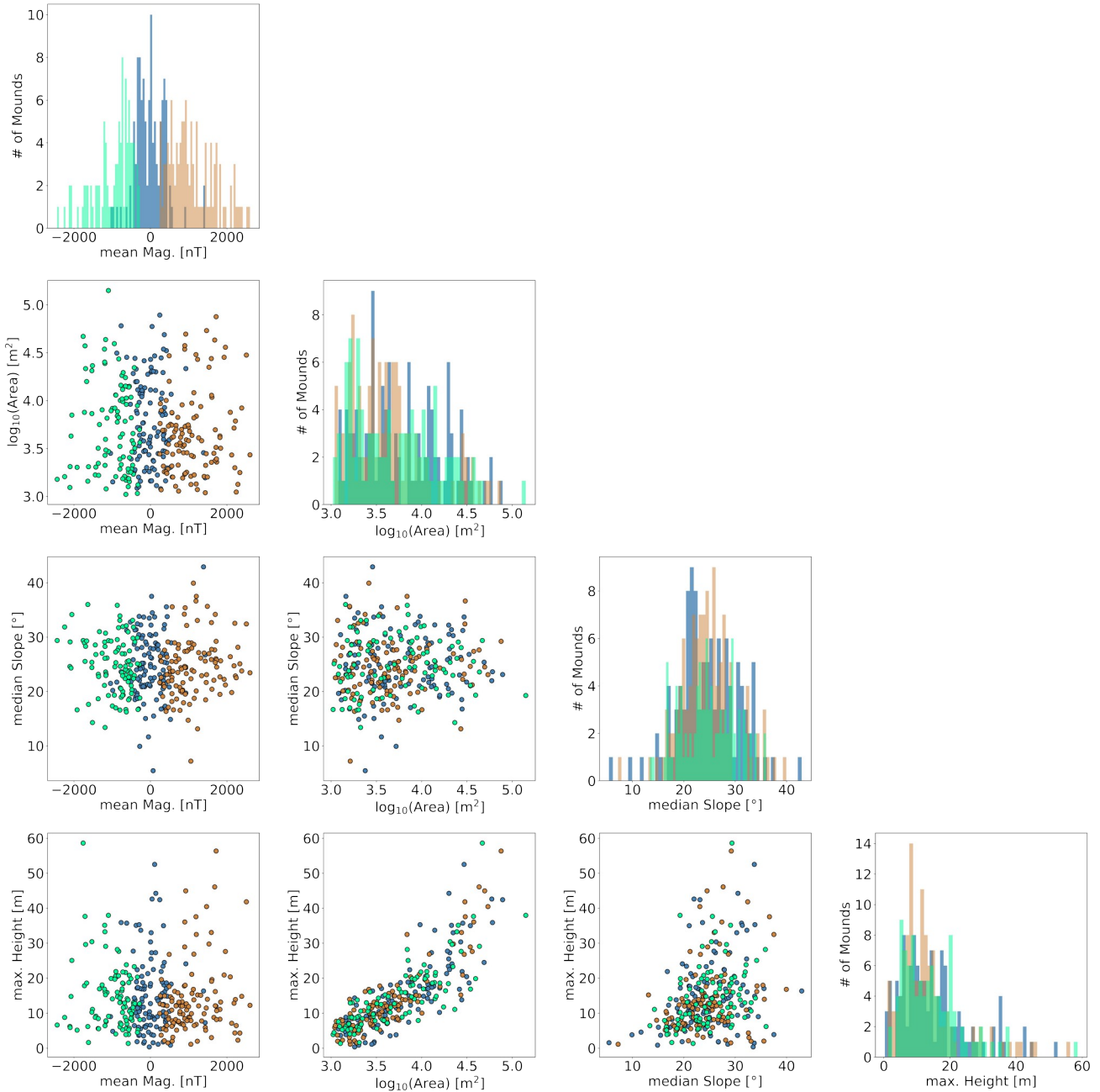


Figure S3: Distribution of morphological and magnetic features for each of the clustered mounds. High, medium and low priority as illustrated in Fig. 9 are shown as green, blue and brown, respectively.